

# Resistive state of SFS Josephson junctions in the presence of moving domain walls

D. S. Rabinovich,<sup>1,2,3</sup> I. V. Bobkova,<sup>3,2</sup> A. M. Bobkov,<sup>3</sup> and M. A. Silaev<sup>4</sup>

<sup>1</sup>*Skolkovo Institute of Science and Technology, Skolkovo 143026, Russia*

<sup>2</sup>*Moscow Institute of Physics and Technology, Dolgoprudny, 141700 Russia*

<sup>3</sup>*Institute of Solid State Physics, Chernogolovka, Moscow reg., 142432 Russia*

<sup>4</sup>*Department of Physics and Nanoscience Center, University of Jyväskylä, P.O. Box 35 (YFL), FI-40014 University of Jyväskylä, Finland*

(Dated: April 9, 2019)

We describe resistive states of the system combining two types of orderings - superconducting and ferromagnetic one. It is shown that in the presence of magnetization dynamics such systems become inherently dissipative and in principle cannot sustain any amount of the superconducting current because of the voltage generated by the magnetization dynamics. We calculate generic current-voltage characteristics of a superconductor/ferromagnet/superconductor Josephson junction with an unpinned domain wall and find the low-current resistance associated with the domain wall motion. We suggest the finite slope of Shapiro steps as the characteristic feature of the regime with domain wall oscillations driven by the ac external current flowing through the junction.

The ability to sustain dissipationless electric currents is assumed to be the defining property of superconducting state. However, this fundamental concept has been challenged by subsequent discovery of type-II superconductors which can be driven into the mixed state characterized by the presence of Abrikosov vortices generated by the magnetic field [1]. The mixed state is generically resistive one since in the absence of additional constraints such as the geometrical confinement of the pinning potential the superconductor vortices start to move under the action of any external current[2]. In such a flux-flow regime vortex motion generates electric field which leads to the finite resistance and Ohmic losses[3, 4].

In this Letter we point out one more fundamental mechanism which can drive superconducting system into the resistive state realized in the ideal situation for arbitrary small applied current. We find that the voltage can be generated in the superconductor-ferromagnet systems due to the interplay of two different order parameters known to produce many non-trivial effects[5–9]. The presence of superconducting condensate allows for the generation of dissipationless spin currents[10] and spin torques to manipulate the magnetic order parameter [8, 9, 11–25]. Here we point out that the magnetization dynamics generated in this way by the supercurrent with necessity generates electric field and Ohmic losses in a way analogous to the Abrikosov vortex motion in the flux-flow regime. However, there is no complete analogy between these fundamental processes. In the case of magnetic system it is the dynamics of magnetic order parameter which is expected to generate electric field and Ohmic losses in the superconducting state due to the Gilbert damping mechanism. The importance of this new resistive state for understanding the physics of non-equilibrium superconducting/ferromagnet systems motivates the present work.

We consider the model system shown in Fig.1 which consists of a Josephson junction between two conven-

tional superconducting leads through a strong ferromagnet. We assume that there is a domain wall (DW) inside the ferromagnetic interlayer. The Rashba-type spin-orbit coupling (SOC) is present in the ferromagnet due to structural or internal inversion symmetry breaking. In Ref. 23 it has been shown that the supercurrent applied to such a system generates a torque on the DW consisting of the adiabatic [26–28] and spin-orbit torques[29, 30]. Under these conditions DW motion is possible even by

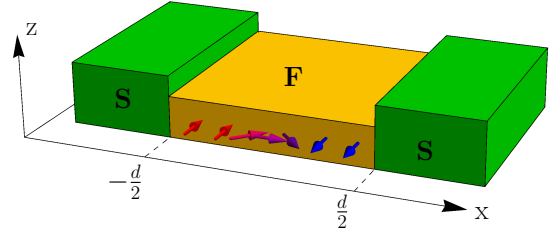


FIG. 1. Sketch of the system under consideration. It is a Josephson junction through a strong ferromagnet in the presence of Rashba SOC. There is a domain wall of Neel type inside the ferromagnetic interlayer.

very small currents if pinning effects are neglected. The DW remains coplanar. In this case due to the absence of nonadiabatic torque in our consideration and coplanarity of the DW the electromotive force [31–36] discussed in the literature before does not occur. Nevertheless, the gauge spin-dependent vector potential appears in the local spin basis due to SOC. It produces the anomalous phase shift and, in case if the magnetization depends on time, it also produces the electromotive force. This situation is the focus of our present study. The electromotive force should be compensated by the voltage induced at the junction. It is this voltage that maintains the DW motion, compensating the dissipation power occurring due to Gilbert damping by the work done by a power source, as it is

shown below.

In principle, if the voltage is induced at the Josephson junction, the quasiparticle distribution in the interlayer becomes nonequilibrium. In this case the non-adiabatic (antidamping) STT[37] can be also produced by the electric current. Here we neglect this effect assuming that the most part of the voltage is dropped at the interfaces and the quasiparticle nonequilibrium in the interlayer is small enough.

*The model and the current-phase relation.* In the considered SFS junction through strong ferromagnet the coupled dynamics of magnetization  $\mathbf{M}$  and Josephson phase difference  $\varphi$  is determined by the following closed set of equations

$$j = j_c \sin(\varphi - \varphi_0\{\mathbf{M}\}) + \frac{\dot{\varphi} - \dot{\varphi}_0\{\mathbf{M}\}}{2eRS}. \quad (1)$$

$$\frac{\partial \mathbf{M}}{\partial t} = -\gamma \mathbf{M} \times \mathbf{H}_{eff} + \frac{\alpha}{M} \mathbf{M} \times \frac{\partial \mathbf{M}}{\partial t} + \mathbf{T}, \quad (2)$$

Eq.(1) represents the non-equilibrium current-phase relation generalizing resistively shunted Josephson junction (RSJ) model. This relation is written in a gauge-invariant form amended to include the anomalous phase shift [12, 24, 38–65]  $\varphi_0\{\mathbf{M}\}$  which is determined by the magnetic texture and SOC. Note that Eq. (1) is applicable even in the normal state that is when  $j_c = 0$ . In contrast to the previously used gauge non-invariant formulations[13, 17] Eq.(1) describes the normal spin-galvanic effects such as the electromotive force and charge current generated in the ferromagnet due to the time derivative of the Berry phase [31–35, 66, 67]. In the Supplementary material [68] we derive Eq.(1) for the generic case of a strong ferromagnetic interlayer with exchange energy splitting being much larger than all other energy scales except of the Fermi energy. In this case only equal-spin triplet correlations survive deep in the interlayer. For a strong ferromagnet the transport can be calculated for spin-up and spin-down Fermi surfaces separately. Then the SU(2) gauge vector potential appears in the local spin basis due to SOC and the magnetic texture reduces to the U(1) gauge field  $\mathbf{Z}$  which is added to the usual electromagnetic vector potential  $\mathbf{A}$  with the opposite effective charges for spin-up and spin-down Fermi-surfaces [59].

Then the anomalous phase shift for the configuration shown in Fig.1 takes the form:

$$\varphi_0\{\mathbf{M}\} = -2 \int_{-d/2}^{d/2} Z_x(x, t) dx. \quad (3)$$

In general, the spin-dependent gauge field is given by the superposition of two terms  $\mathbf{Z} = \mathbf{Z}^m + \mathbf{Z}^{so}$ .  $\mathbf{Z}_i^m = -i \text{Tr}(\hat{\sigma}_z \hat{U}^\dagger \partial_i \hat{U})/2$  is the texture-induced part, where  $\hat{U}(\mathbf{r}, t)$  is the time- and space-dependent unitary

$2 \times 2$  matrix that rotates the spin quantization axis  $z$  to the local frame determined by the exchange field.

The term  $\mathbf{Z}_j^{so} = (M_i B_{ij})/M$  appears due to the SOC, where  $B_{ij}$  is the constant tensor coefficient describing the linear spin-orbit coupling of the general form  $\hat{H}_{so} = \sigma_i B_{ij} p_j/m$ . Here we assume that  $\hat{H}_{so}$  is of Rashba type:  $\hat{H}_{so} = (B_R/m)(\sigma_x p_y - \sigma_y p_x)$ .  $\mathbf{Z}^m$  only nonzero for non-coplanar magnetic structures. For the case under consideration the DW is assumed to be moved as a plane object, consequently  $\mathbf{Z}^m = 0$ . The spin-orbit part is the only source of the spin-dependent gauge field in our case [76].

The magnetization dynamics driven by the spin-polarized supercurrent is described by LLG Eq.(2) where  $\alpha$  is the Gilbert damping constant,  $\gamma$  is the gyromagnetic ratio. The last term in Eq.(2) is the current-induced spin torque  $\mathbf{T} = (\gamma/M)(\mathbf{J}_s \nabla) \mathbf{M} + (2\gamma/M)(\mathbf{M} \times \mathbf{B}_j) \mathbf{J}_{s,j}$ . The first term here is the adiabatic spin-transfer torque generated by the spin current which has the amplitude  $\mathbf{J}_s$  in the local spin basis. The second term is the spin-orbit induced torque determined by the spin vector  $\mathbf{B}_j = (B_{xj}, B_{yj}, B_{zj})$  corresponding to the  $j$ -th spatial component of the SOC tensor  $B_{ij}$  and  $\mathbf{J}_s$  is the spin current. Below we assume  $R_\uparrow \ll R_\downarrow$  and neglect for simplicity the spin-down contribution to the current. In this case  $\mathbf{J}_s \approx \mathbf{j}/2e$ .

To study DW motion magnetization  $\mathbf{M} = M(\sin \theta \sin \delta, \cos \theta, \sin \theta \cos \delta)$ , where the both angles depend on  $(x, t)$ , can be found from LLG Eq.(2).

At zero applied supercurrent the equilibrium shape of the DW is given by  $\delta = \pi/2$  and

$$\cos \theta = -\tanh[(x - x_0)/d_W], \quad (4)$$

where  $d_W = \sqrt{A_{ex}/K}$  is the DW width. Here it is assumed that  $K > 0$  and  $K_\perp > 0$  are the anisotropy constants for the easy and hard axes, respectively and  $A_{ex}$  is the constant describing the inhomogeneous part of the exchange energy. The effective magnetic field  $\mathbf{H}_{eff} = (1/M^2)(K M_y \mathbf{y} - K_\perp M_z \mathbf{z} + A_{ex} \partial_x^2 \mathbf{M})$ .

It was shown in Ref. 23 that the spin-orbit torque induced by the Rashba-type SOC moves the Neel DW at small currents without any threshold. All the results discussed in the present paper are also valid for a head-to-head DW with the bulk magnetization pointing along the  $x$ -axis. But here it is the Dresselhaus SOC that plays the "active part" in motion of the DW. It was demonstrated [23] that this problem is mathematically equivalent to the problem of the Neel DW, described above, in the presence of the Rashba SOC-induced torque.

For dealing with the SOC-induced torque it is convenient to define the dimensionless SOC constant  $\beta = -2B_R d_W$ . For small applied supercurrents  $j \ll d_W M e / (t_d \mu_B |\alpha - \beta|)$  the DW wall moves as a coplanar object corresponding to  $\theta(x, t)$  defined by Eq. (4) with

$x_0(t) = \int_{t_0}^t v(t') dt'$  and  $\delta \equiv \delta(t)$ . The exact solution for  $v(t)$  following from Eq. (2) for the situation when the electric current is switched on at  $t = 0$  is presented in the Supplementary material[68]. Physically, the velocity gradually reaches its stationary value  $v_{st}$  on a characteristic time scale  $t_d = (1 + \alpha^2)M/(\alpha\gamma K_\perp)$ . This stationary value takes the form

$$v_{st} = -\frac{u\beta}{\alpha}, \quad (5)$$

where  $u = \gamma J_s/M$  is the characteristic velocity associated with a given value of spin current flowing through the ferromagnetic interlayer.

In the considered case of Neel DW and Rashba SOC  $Z_x^{so} = (\beta M_y)/(2d_W M)$ . Substituting the last expression into Eq. (3) we obtain the following answer for the anomalous phase shift:

$$\varphi_0(t) \approx -2\beta x_0(t)/d_W. \quad (6)$$

Our consideration is strictly applicable if  $|d/2 \pm x_0| \gg d_W$ , that is if the DW is not close to the S/F interface.

*Resistive state.* Suppose that we apply a constant electric current  $I = jS$  to the Josephson junction and consider a steady motion of the DW across the junction with a constant velocity defined by Eq. (5). In this case Eq. (1) can be easily solved and the time-averaged voltage induced at the junction is

$$\overline{V(t)} = RS\sqrt{j^2 - j_c^2} + \frac{\beta^2 u}{e\alpha d_W}, \quad (7)$$

where the first term represents the well-known Josephson voltage, which is generated at  $j > j_c$ . The second term is nonzero as at  $j > j_c$ , so as at  $j < j_c$  and reflects the fact that the Josephson junction is in the resistive state if the DW is moved by the current. The corresponding IV-characteristics of the junction are shown in Fig. 2.

The resistance of the junction at  $j < j_c$  caused by the DW motion is given by

$$R_{DW} = \left( \frac{\partial V}{\partial I} \right)_{I < I_c} = \frac{\mu_B \beta^2 \hbar}{e^2 S \alpha d_W M}. \quad (8)$$

It is interesting that according to Eq. (8)  $R_{DW}$  per unit area does not depend on the Josephson junction parameters, such as  $j_c$  and  $R$ , and is determined only by the characteristics of the magnetic subsystem. It can be naturally understood if we take into account that in this case the work done by a power source is exactly equal to the energy losses due to the Gilbert damping. Indeed, the dissipation power due to Gilbert damping can be calculated as [69]

$$P_G = \frac{\alpha}{\gamma M} \int dx \left( \frac{d\mathbf{M}}{dt} \right)^2 \quad (9)$$

It can be easily calculated that the magnetization described by Eq. (4) corresponding to the stationary DW

motion with  $\dot{x}_0 = v_{st}$  results in the following answer for the dissipation power

$$P_G = \frac{u\beta^2}{e\alpha d_W} j, \quad (10)$$

what exactly coincides with the power  $jV$  provided by the source.

Therefore, in the regime  $j < j_c$  the normal current through the Josephson junction is zero in spite of nonzero voltage generated at the junction. It can be also easily seen directly from Eq. (1) because the solution of this equation for  $j < j_c$  takes the form  $\dot{\varphi}(t) = \dot{\varphi}_0(t)$ . The equivalent circuit scheme of the junction is presented in the insert to Fig. 2. The voltage is compensated by the electromotive force induced in the junction by the emergent electric field  $(\hbar/e)\mathbf{Z}_{so}$ .

If there are  $n$  DWs inside the junction, when under the assumptions above  $R_{DW}$  expressed by Eq. (8) is multiplied by  $n$ . If the Josephson junction is driven by an ac component of the voltage or current having the frequency  $\omega$ , then the dependence  $V(I)$  manifest horizontal steps at  $V_k = k\omega/2e$ , which are known as the Shapiro steps[70, 71]. If a moving DW is present in the junction the Shapiro steps acquire a nonzero slope, which is determined by Eq. (8). The reason is that in this case the oscillation frequency of the Josephson current is determined by  $\overline{\dot{\varphi}} - \dot{\varphi}_0$  and does not coincide with  $2eV$  anymore. The Shapiro steps occur just when the oscillation frequency of the Josephson current equals to multiple integer of the external frequency. The IV-characteristic demonstrating the inclined Shapiro steps is shown in the insert to Fig. 2.

In real setups the time of the DW movement through the junction is limited by the finite junction length:  $t_{DW} \approx d/v_{st} = (\alpha/\beta)(d/u)$ . Therefore, the voltage should be averaged over  $t < t_{DW}$ . Although experimental data on the DW motion in Josephson junctions has not been available yet, for the estimates we take  $d = 0.5 \times 10^{-6}$  m and  $u \leq u_{max} \approx 1$  m/s, where  $u_{max}$  corresponds to the maximal Josephson current density[72] through the CrO<sub>2</sub> nanowire  $j_c \sim 10^9$  A/m<sup>2</sup>. Then  $t_{DW} \geq 0.5(\alpha/\beta) \times 10^{-6}$ s. For other experiments, where the Josephson current carried by equal-spin triplet correlations was reported [73, 74], this time can be several orders of magnitude higher due to much less values of the critical current density.

The IV-characteristic presented in Fig. 2 was obtained under the assumption of a steady DW motion. In fact,  $V(t)$  is driven by  $\dot{\varphi}_0 \sim v(t)$ . For a step-like applied electric current  $V(t)$  saturates exponentially at the characteristic time  $t_d$  except for the short Josephson pulses (see below). Therefore, in order to be able to measure the resistance expressed by Eq. (8) it is important to have  $t_{DW} > t_d$ . For estimations of  $t_d$  we use the material parameters of the CrO<sub>2</sub> nanostructures [72, 75]. Taking the saturation magnetization  $M = 4.75 \times 10^5$  A/m,  $K =$

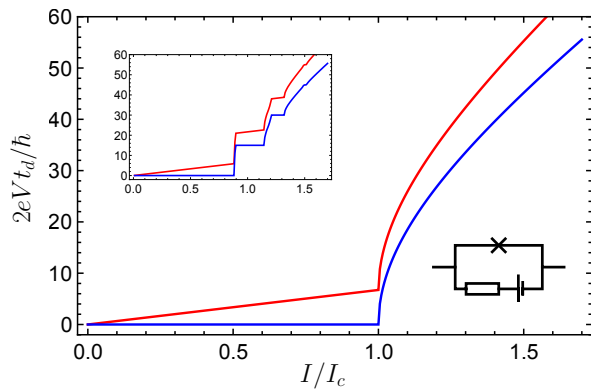


FIG. 2. IV-characteristics of the SFS junction with a DW at rest (blue) and a moving DW (red).  $\beta = 1$ ,  $\alpha = 0.1$ ,  $eKd_W = 5j_c$ ,  $t_d = 40t_J$ , where  $t_J = 1/2eRI_c$ . Upper-left insert: Shapiro steps for  $I(t) = I + 0.3I_c \cos \omega t$ ,  $\omega = 15t_d^{-1}$ . Axes labelling is the same as in the main figure. Bottom-right insert: the equivalent circuit scheme of the junction.

$1.43 \times 10^5 \text{ erg/cm}^3$  and  $K_{\perp} = 4\pi M^2$ ,  $\alpha = 0.01$  we obtain  $t_d \approx 10^{-9} \text{ s}$ . Consequently, the ratio  $t_{DW}/t_d > 1/\beta$  and for not very large values of the SOC constant  $\beta \lesssim 1$  the condition  $t_{DW} > t_d$  is realistic.

In practice DW motion can be induced by large current pulses. For short pulses  $j(t) = j\theta(t)\theta(T-t)$  with  $T < t_{DW}$ , the DW does not go out of the junction during the impulse time. The exact expression for the DW velocity  $v(t)$  is to be found from the LLG equation and is calculated in the Supplementary material[68]. The resulting voltage signal consists of two parts of different physical origin. The first part is the purely Josephson response with the characteristic time  $t_J = 1/2eRI_c$  and the other part is of purely magnetic origin, has time scale  $t_d$  and vanishes if there is no a moving DW in the junction. Taking for estimations of  $t_J$  the material parameters of the  $\text{CrO}_2$  nanostructures  $j_c \sim 10^9 \text{ A/m}^2$ ,  $R \sim 0.3-1.5\Omega$ ,  $S = 7.5 \times 10^{-14} \text{ m}^2$  we obtain  $t_J = 0.3 \times 10^{-11} - 1.5 \times 10^{-11} \text{ s}$ . According to this estimate  $t_J \ll t_d$ . Then the Josephson voltage signal should decay much faster than the DW signal.

The resulting dependence of the voltage signal on time is shown in Fig. 3. In Fig. 3(a)  $V(t)$  is demonstrated at  $j < j_c$ . Different curves correspond to different impulse periods  $T$ . It is seen that a typical  $V(t)$  curve consists of an initial sharp Josephson voltage impulse decaying at  $t \sim t_J$ , a final sharp impulse of the same nature and a gradual voltage increase and decrease of purely magnetic origin, which takes the form

$$V(t) = -\frac{2\beta v(t)}{d_W}. \quad (11)$$

It saturates at time  $t_d$  to the voltage defined by the steady DW motion velocity. The dashed curves correspond to the same rectangular voltage impulse, but with no moving DW inside the interlayer. It is seen that they exhibit

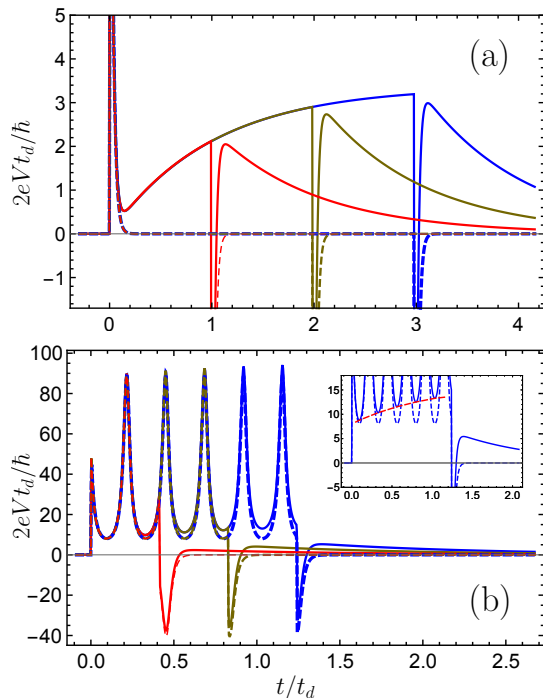


FIG. 3.  $V(t)$  for rectangular current impulses. Different curves correspond to different impulse periods  $T$ ; For all the panels the solid lines correspond to  $\beta = 1$  (the anomalous phase due to the DW motion is nonzero) and the dashed lines are for  $\beta = 0$  (the anomalous phase shift is zero). (a)  $j = 0.5j_c$ ,  $T = 3t_d$  (blue),  $T = 2t_d$  (yellow),  $T = t_d$  (red); (b)  $j = 1.2j_c$ ,  $T = 1.25t_d$  (blue),  $T = 0.83t_d$  (yellow),  $T = 0.42t_d$  (red). Insert:  $j = 1.2j_c$ ,  $T = 1.25t_d$  (the part of the main panel on a large scale); For all the curves  $\alpha = 0.1$ ,  $eKd_W = 5j_c$ ,  $t_d = 40t_J$ .

no finite voltage between the initial and final Josephson pulses.

Fig. 3(b) demonstrates  $V(t)$  at  $j > j_c$ . The difference with the previous case is that the voltage exhibit Josephson oscillations during the impulse time. Nevertheless, the gradual increase of the voltage due to the DW motion is also present. It is seen as an increasing difference between the solid and the dashed minima in the main figure and in the insert, what is marked by a red dashed line.

To conclude we have generalized the RSJ equation to describe the new resistive state generated by magnetization dynamics in the interlayer of a S/F/S junction. Taking into account the emergent vector potential originated from SOC and/or magnetization texture we obtained the gauge-invariant system of coupled equations which governs the dynamics of magnetization and superconducting phase. Using this model we have shown that in the presence of magnetization dynamics the Josephson junction is in the resistive state even at  $j < j_c$ . In this regime the junction can be used for electrical detection

of the dynamics. Experimentally DW motion inside the Josephson junction can be observed through the nonzero slope of Shapiro steps.

*Acknowledgements.* The research of I.V.B and A.M.B has been carried out within the state task of ISSP RAS with the support by RFBR grant 19-02-00466. D.S.R acknowledges the support by RFBR grants 19-02-00466 and 19-02-00898. The work of M.A.S was supported by the Academy of Finland (Project No. 297439)

## SUPPLEMENTARY MATERIAL

### Derivation of the modified RSJ equation

For the system under consideration the interlayer is assumed to be made of a strong ferromagnet and can be described by the Green's function  $\hat{g}_\sigma$ , defined at spin-up and spin-down Fermi surfaces separately, which is a  $4 \times 4$  matrix in the particle-hole and Keldysh spaces, but is a scalar in spin space. In the local reference frame, where the spin quantization axis is aligned with the local direction of the exchange field in the ferromagnet it obeys the following generalized Eilenberger-Keldysh equation [23, 59]

$$-iD_\sigma \hat{\partial}_{\mathbf{R}}(\hat{g}_\sigma \otimes \hat{\partial}_{\mathbf{R}}\hat{g}_\sigma) + [\varepsilon\hat{\tau}_3, \hat{g}_\sigma]_\otimes = 0, \quad (12)$$

where  $\tau_i$  are Pauli matrices in the particle-hole space, the  $\otimes$ -product is defined as  $\hat{A}(\varepsilon, t) \otimes \hat{B}(\varepsilon, t) = \exp[(i/2)(\partial_{\varepsilon_A} \partial_{t_B} - \partial_{\varepsilon_B} \partial_{t_A})] \hat{A}(\varepsilon, t) \hat{B}(\varepsilon, t)$ . The operator  $\hat{\partial}_{\mathbf{R}}$  means the covariant derivative  $\hat{\partial}_{\mathbf{R}} = \partial_{\mathbf{R}} + i\sigma[Z\tau_3, \dots]_\otimes$  with  $[\hat{A}, \hat{B}]_\otimes = \hat{A} \otimes \hat{B} - \hat{B} \otimes \hat{A}$ .  $\mathbf{Z}$  is the U(1) gauge field which is added to the usual electromagnetic vector potential  $\mathbf{A}$  with the opposite effective charges for spin-up and spin-down Fermi-surfaces[59]. In general, the spin-dependent gauge field is given by the superposition of two terms  $\mathbf{Z} = \mathbf{Z}^m + \mathbf{Z}^{so}$ .  $Z_i^m = -i\text{Tr}(\hat{\sigma}_z \hat{U}^\dagger \partial_i \hat{U})/2$  is the texture-induced part, where  $\hat{U}(\mathbf{r}, t)$  is the time- and space-dependent unitary  $2 \times 2$  matrix that rotates the spin quantization axis  $z$  to the local frame determined by the exchange field.

The term  $Z_j^{so} = (M_i B_{ij})/M$  appears due to SOC, where  $B_{ij}$  is the constant tensor coefficient describing the linear SOC of the general form  $\hat{H}_{so} = \sigma_i B_{ij} p_j/m$ . Here we assume that  $\hat{H}_{so}$  is of Rashba type:  $\hat{H}_{so} = (B_R/m)(\sigma_x p_y - \sigma_y p_x)$ .  $\mathbf{Z}^m$  only nonzero for noncoplanar magnetic structures. For the case under consideration the DW is assumed to be moved as a plane object, consequently  $\mathbf{Z}^m = 0$ . The spin-orbit part is the only source of the spin-dependent gauge field in our case.

The general expression for the electric current inside the strong ferromagnet can be written as a sum over two

spin subbands [23]:

$$j = \frac{e}{8} \sum_\sigma \nu_\sigma D_\sigma \text{Tr}_2 \int [\tau_3 \hat{g}_\sigma \otimes \hat{\partial}_x \hat{g}_\sigma]^K d\varepsilon, \quad (13)$$

where  $\nu_\sigma$  and  $D_\sigma$  are the density of states at the Fermi level and the diffusion constant for a given spin subband.  $[\dots]^K$  means the Keldysh component of the corresponding matrix.

In general, the current can be viewed as a sum of supercurrent and a normal current, carried by quasiparticles. Here we consider high-temperature limit  $\Delta(T) \ll T_c$  and linear response theory. We only keep the leading order terms in expressions for supercurrent and for normal current. This means that the supercurrent is calculated with the equilibrium distribution function neglecting nonequilibrium corrections and the normal current is calculated in the linear order with respect to the potential drop  $V$  and for  $\Delta \rightarrow 0$ . Therefore, we neglect the terms of the order  $(\Delta^2/T_c^2)(eV/T_c)$  upon the current calculation. The supercurrent in the framework of this approximation has been already calculated [59] and is represented by the first term of Eq. (1) of the main text. Here we are only interested in the expression for the normal current in the presence of the emergent electric field induced by the SO coupling in the weak link of the junction. At  $\Delta \rightarrow 0$   $\hat{g}_\sigma^{R,A} = \pm\tau_3$  and  $\hat{g}_\sigma^K = 2\tau_3 \hat{\varphi}_\sigma$ , where  $\hat{\varphi}_\sigma = \varphi_\sigma^e(1 + \tau_3)/2 + \varphi_\sigma^h(1 - \tau_3)/2$  is the quasiparticle distribution function for a given spin subband. Eq. (13) is simplified as follows:

$$j = \frac{e}{2} \sum_\sigma \nu_\sigma D_\sigma \int \hat{\partial}_x \varphi_\sigma^e d\varepsilon. \quad (14)$$

$$\begin{aligned} \hat{\partial}_x \varphi_\sigma^e &\approx \partial_x \varphi_\sigma - \frac{\sigma}{2} (\partial_{\varepsilon_1} \partial_{t_2} - \partial_{\varepsilon_2} \partial_{t_1}) \times \\ & \left[ Z_x^{so}(t_1) \varphi_\sigma(\varepsilon_2) - Z_x^{so}(t_2) \varphi_\sigma(\varepsilon_1) \right] \Big|_{\varepsilon_1=\varepsilon_2=\varepsilon; t_1=t_2=t} = \\ & \partial_x \varphi_\sigma^e + \sigma \partial_\varepsilon \varphi_\sigma^e \dot{Z}_x^{so} \end{aligned} \quad (15)$$

Assuming that the quasiparticle nonequilibrium in the interlayer can be described by the Fermi distribution function with a spatially-dependent electric potential  $\varphi_\sigma = \tanh[(\varepsilon - eV_\sigma(x))/2T]$  we can further simplify Eq. (15):

$$\hat{\partial}_x \varphi_\sigma^e \approx \partial_\varepsilon \varphi_\sigma^e (-e\partial_x V_\sigma + \sigma \dot{Z}_x^{so}). \quad (16)$$

Substituting Eq. (16) into Eq. (14) one can obtain

$$j = -e \sum_\sigma \nu_\sigma D_\sigma (e\partial_x V_\sigma - \sigma \dot{Z}_x^{so}). \quad (17)$$

Assuming that the interlayer is a half-metal, that is the density of states is nonzero only for one of the spin subbands, we obtain from Eq. (17) that the potential gradient in the interlayer takes the form:

$$e\partial_x V = -\frac{j}{e\nu D} + \dot{Z}_x^{so}. \quad (18)$$

Let us choose the electric potential in the left electrode to be zero  $V_L = 0$ . Then the electric potential of the right electrode

$$V_R = V_{L,b} + V_{int} + V_{R,b}, \quad (19)$$

where  $V_{L(R),b} = -jR_{L(R)}$  is the potential jump at the left (right) S/F interface and  $V_{int} = \int_{-d/2}^{d/2} \partial_x V dx$  is the potential difference acquired inside the interlayer.

Substituting Eq. (18) into Eq. (19) we obtain

$$j = \frac{-(V_R - V_L) + (1/e) \int_{-d/2}^{d/2} \dot{Z}_x^{so} dx}{R}, \quad (20)$$

where we have introduced the total normal resistance of the junction  $R = R_L + R_R + d/(e^2 \nu D)$ .

Recalling that  $V_L - V_R = \dot{\varphi}/2e$  and  $\dot{\varphi}_0 = -2 \int_{-d/2}^{d/2} \dot{Z}_x^{so} dx$  we finally obtain

$$j_n = \frac{\dot{\varphi} - \dot{\varphi}_0}{2eR}. \quad (21)$$

### DW motion induced by a given current profile

Here we derive exact expressions for the DW velocity as a function of time for different current regimes considered in the main text. The full dependence  $v(t)$  can be obtained starting from the LLG equation (2). Substituting  $\cos \theta$  in the form of Eq. (4) and  $\delta = \delta_0 + \Delta\delta(t)$ , where  $\delta_0 = \pi/2$  for a Neel DW, into Eq. (2), assuming  $\Delta\delta \ll 1$  and keeping only first order terms with respect to this parameter, after some algebra we obtain the following expression for  $v(t)$ :

$$v(t) = \exp(-t/t_d) \times \int_{-0}^t \exp(t'/t_d) \left( -u(t') \frac{\beta}{\alpha t_d} + u'(t') \frac{1 - \alpha\beta}{1 + \alpha^2} \right) dt', \quad (22)$$

where  $t_d = (1 + \alpha^2)M/\alpha\gamma K_\perp$  and  $u(t) = \gamma j(t)/2eM$ . Eq. (22) is valid for an arbitrary dependence of  $j(t)$  if the current is switched on at  $t = 0$ .

If a constant current  $j(t) = j\theta(t)$  is switched on at  $t = 0$ , then one can obtain from Eq. (22) that at  $t > 0$

$$v(t) = \frac{e^{-t/t_d} u}{1 + \alpha^2} \left( 1 + \frac{\beta}{\alpha} \right) - \frac{\beta u}{\alpha}. \quad (23)$$

As it was stated in the main text, the DW velocity at  $t > 0$  saturates exponentially to the value  $v_{st}$  defined by Eq. (5).

For the case of a rectangular current impulse  $j(t) = j\theta(t)\theta(T - t)$  the DW velocity takes the form:

$$v(t) = -\exp(-t/t_d)\theta(t) \frac{\mu_B j}{eM} \left[ \frac{\alpha + \beta}{\alpha(1 + \alpha^2)} \times \left( \exp(T/t_d)\theta(t - T) - 1 \right) + \frac{\beta}{\alpha} \exp(t/t_d)\theta(T - t) \right] \quad (24)$$

### Voltage induced by a rectangular current impulse

Having at hand the dependence  $v(t)$  one can find the anomalous phase shift as a function of time. According to Eq. (6) of the main text

$$\varphi_0(t) \approx -2\beta/d_W \int_0^t v(t') dt'. \quad (25)$$

Solving Eq. (1) with  $j(t) = j\theta(t)\theta(T - t)$  and  $\varphi_0(t)$  defined by Eqs. (25) and (24) we obtain:

$$\dot{\varphi}(t) = \frac{\Omega \left( \frac{j}{j_c} - 1 \right) \theta(T - t)}{\frac{j}{j_c} - \cos(\Omega t \sqrt{(j/j_c)^2 - 1} + \arctan \sqrt{(j/j_c)^2 - 1}) - \frac{2\Omega D \exp(-\Omega t)\theta(t - T)}{1 + D^2 \exp(-2\Omega t)} - \frac{2\beta v(t)}{d_W}}, \quad (26)$$

where  $D = (j_c/j) \exp(\Omega T) (1 - \sqrt{(j/j_c)^2 - 1}) \times \cot(\Omega T \sqrt{(j/j_c)^2 - 1}/2 + \arctan \sqrt{(j/j_c)^2 - 1})$ ,  $\Omega = t_J^{-1} = 2eRI_c$ . At  $j < j_c$   $\sqrt{(j/j_c)^2 - 1} \rightarrow i\sqrt{1 - (j/j_c)^2}$ .  $V(t)$  described by Eq. (26) is plotted in Fig. 3 of the main text.

- 
- [1] A. A. Abrikosov, Zh. Eksperim. i Teoret. Fiz. **32**, 1442 (1957) [Soviet Phys. JETP **6**, 1174 (1957)].
  - [2] Y. B. Kim, C. F. Hempstead, and A. R. Strnad, Phys. Rev. **139**, A1163 (1965).
  - [3] J. Bardeen and M. J. Stephen, Phys. Rev. **140**, A1197 (1965).
  - [4] L. P. Gorkov and N. B. Kopnin, Soviet Physics Uspekhi **18**, 496 (1975).
  - [5] F. S. Bergeret, A. F. Volkov, K. B. Efetov, Rev. Mod. Phys. **77**, 1321 (2005).
  - [6] A. I. Buzdin, Rev. Mod. Phys. **77**, 935 (2005)
  - [7] F. S. Bergeret, M. Silaev, P. Virtanen, and T. T. Heikkilä, Rev. Mod. Phys. **90**, 041001 (2018)
  - [8] M. Eschrig, T. Lofwander, Nat. Phys. **4**, 138 (2008).
  - [9] M. Houzet, A. I. Buzdin, Phys. Rev. B **76**, 060504(R) (2007).
  - [10] M. Eschrig, Rep. Prog. Phys. **78**, 104501 (2015)
  - [11] Waintal and P. W. Brouwer, Phys. Rev. B **65**, 054407 (2002).
  - [12] A.I. Buzdin, Phys. Rev. Lett. **101**, 107005 (2008).
  - [13] F. Konschelle, A. Buzdin Phys. Rev. Lett. **102**, 017001 (2009)
  - [14] S. Teber, C. Holmqvist, and M. Fogelström, Phys. Rev. B **81**, 174503 (2010)

- [15] C. Holmqvist, W. Belzig, and M. Fogelstrom, *Phys. Rev. B* **86**, 054519 (2012)
- [16] J. Linder and T. Yokoyama, *Phys. Rev. B* **83**, 012501 (2011).
- [17] Yu. M. Shukrinov, I. R. Rahmonov, K. Sengupta, and A. Buzdin, *Appl. Phys. Lett.* **110**, 182407 (2017).
- [18] E. M. Chudnovsky, *Phys. Rev. B* **93**, 144422 (2016).
- [19] V. Braude and Ya. M. Blanter, *Phys. Rev. Lett.* **100**, 207001 (2008).
- [20] Z. Nussinov, A. Shnirman, D. P. Arovas, A. V. Balatsky, and J.-X. Zhu, *Phys. Rev. B* **71**, 214520 (2005)
- [21] J.-X. Zhu, Z. Nussinov, A. Shnirman, and A. V. Balatsky, *Phys. Rev. Lett.* **92**, 107001 (2004)
- [22] L. Cai and E. M. Chudnovsky, *Phys. Rev. B* **82**, 104429 (2010).
- [23] I. V. Bobkova, A. M. Bobkov, and M.A. Silaev, *Phys. Rev. B* **98**, 014521 (2018).
- [24] D.S. Rabinovich, I.V. Bobkova, A.M. Bobkov and M.A. Silaev, *Phys. Rev. B* (2018).
- [25] F. Aikebaier, P. Virtanen, and T.T. Heikkila, *Phys. Rev. B* **99**, 104504 (2019)
- [26] J. C. Slonczewski, *Journal of Magnetism and Magnetic Materials* **159**, L1 (1996).
- [27] G. Tatara and H. Kohno, *Phys. Rev. Lett.* **92**, 086601 (2004).
- [28] T. Koyama, D. Chiba, K. Ueda, K. Kondou, H. Tanigawa, S. Fukami, T. Suzuki, N. Ohshima, N. Ishiwata, Y. Nakatani, K. Kobayashi, and T. Ono, *Nature Materials* **10**, 194 (2011).
- [29] I. M. Miron, G. Gaudin, S. Auffret, B. Rodmacq, A. Schuhl, S. Pizzini, J. Vogel, and P. Gambardella, *Nature Mater.* **9**, 230 (2010).
- [30] P. Gambardella and I. M. Miron, *Philos Transact A Math Phys Eng Sci* **369**, 3175 (2011).
- [31] G. E. Volovik, *J. Phys. C* **20**, L83 (1987).
- [32] S.E. Barnes and S. Maekawa, *Phys. Rev. Lett.* **98**, 246601 (2007).
- [33] W. M. Saslow, *Phys. Rev. B* **76**, 184434 (2007).
- [34] R. A. Duine, *Phys. Rev. B* **77**, 014409 (2008).
- [35] Y. Tserkovnyak and M. Mecklenburg, *Phys. Rev. B* **77**, 134407 (2008).
- [36] S. Zhang and S. S.-L. Zhang, *Phys. Rev. Lett.* **102**, 086601 (2009).
- [37] S. Zhang and Z. Li, *Phys. Rev. Lett.* **93**, 127204 (2004).
- [38] Y. Asano, Y. Sawa, Y. Tanaka, and A.A. Golubov, *Phys. Rev. B* **76**, 224525 (2007).
- [39] A.A. Reynoso, G. Usaj, C.A. Balseiro, D. Feinberg, and M. Avignon, *Phys. Rev. Lett.* **101**, 107001 (2008).
- [40] Y. Tanaka, T. Yokoyama and N. Nagaosa, *Phys. Rev. Lett.* **103**, 107002 (2009).
- [41] R. Grein, M. Eschrig, G. Metalidis, and G. Schon, *Phys. Rev. Lett.* **102**, 227005 (2009).
- [42] A. Zazunov, R. Egger, T. Jonckheere, and T. Martin, *Phys. Rev. Lett.* **103**, 147004 (2009).
- [43] J.-F. Liu, K. S. Chan, *Phys. Rev. B* **82**, 184533 (2010).
- [44] A.G. Malshukov, S. Sadjina, and A. Brataas, *Phys. Rev. B* **81**, 060502 (2010).
- [45] M. Alidoust and J. Linder, *Phys. Rev. B* **87**, 060503(R) (2013).
- [46] A. Brunetti, A. Zazunov, A. Kundu, and R. Egger *Phys. Rev. B* **88**, 144515 (2013).
- [47] T. Yokoyama, M. Eto, and Yu. V. Nazarov, *Phys. Rev. B* **89**, 195407 (2014).
- [48] I. Kulagina and J. Linder, *Phys. Rev. B* **90**, 054504 (2014).
- [49] A. Moor, A.F. Volkov, and K.B. Efetov, *Phys. Rev. B* **92**, 214510 (2015).
- [50] A. Moor, A. F. Volkov, and K. B. Efetov, *Phys. Rev. B* **92**, 180506 (2015).
- [51] F. S. Bergeret and I. V. Tokatly, *EPL* **110**, 57005 (2015).
- [52] G. Campagnano, P. Lucignano, D. Giuliano and A. Tagliacozzo, *J. Phys. Cond. Mat.* **27**, 205301 (2015).
- [53] S. Mironov and A. Buzdin, *Phys. Rev. B* **92**, 184506 (2015).
- [54] F. Konschelle, I. V. Tokatly, and F. S. Bergeret, *Phys. Rev. B* **92**, 125443 (2015).
- [55] D. Kuzmanovski, J. Linder, A. Black-Schaffer, *Phys. Rev. B* **94**, 180505 (2016).
- [56] A. A. Zyuzin, M. Alidoust, and D. Loss, *Phys. Rev. B* **93**, 214502 (2016).
- [57] I. V. Bobkova, A. M. Bobkov, A. A. Zyuzin, and M. Alidoust, *Phys. Rev. B* **94**, 134506 (2016).
- [58] M. A. Silaev, I. V. Tokatly, and F. S. Bergeret, *Phys. Rev. B* **95**, 184508 (2017).
- [59] I.V. Bobkova, A.M. Bobkov, and M.A. Silaev, *Phys. Rev. B* **96**, 094506 (2017).
- [60] D.B. Szombati, S. Nadj-Perge, D. Car, S. R. Plissard, E. P. A. M. Bakkers, and L. P. Kouwenhoven, *Nature Phys.* **12**, 568 (2016).
- [61] A. Murani, A. Kasumov, S. Sengupta, Yu. A. Kasumov, V.T. Volkov, I. I. Khodos, F. Brisset, R. Delagrange, A. Chepelienskii, R. Deblock, H. Bouchiat, and S. Guron, *Nature Comm.* **8**, 15941 (2017).
- [62] A. Assouline, C. Feuillet-Palma, N. Bergeal, T. Zhang, A. Mottaghizadeh, A. Zimmers, E. Lhuillier, M. Marangolo, M. Eddrief, P. Atkinson, M. Aprili, and H. Aubin, *arXiv:1806.01406*.
- [63] H. Meng, A. V. Samokhvalov, and A. I. Buzdin, *PRB* **99**, 024503 (2019)
- [64] I.V. Krive, L.Y. Gorelik, R.I. Shekhter, and M. Jonson, *Phys. Nizk. Temp.* **30**, 535 (2004).
- [65] V. Braude and Yu.V. Nazarov, *Phys. Rev. Lett.* **98**, 077003 (2007).
- [66] T. Schulz et al., *Nature Physics* **8**, 301 (2012)
- [67] N. Nagaosa, Y. Tokura, *Nature Nanotechnology* **8**, 899 (2013)
- [68] See supplementary material at...
- [69] Y. Tserkovnyak and C. H. Wong, *Phys. Rev. B* **79**, 014402 (2009).
- [70] S. Shapiro, *Phys. Rev. Lett.* **11**, 80 (1963).
- [71] C. C. Grimes and S. Shapiro, *Phys. Rev.* **169**, 397 (1968).
- [72] A. Singh, C. Jansen, K. Lahabi, and J. Aarts, *Phys. Rev. X* **6**, 041012 (2016).
- [73] T.S. Khaire, M. A. Khasawneh, W. P. Pratt, Jr., and N. O. Birge, *Phys. Rev. Lett.* **104**, 137002 (2010).
- [74] J. W. A. Robinson, J. D. S. Witt, M. G. Blamire, *Science* **329**, 59 (2010).
- [75] X. Zou and G. Xiao, *Appl. Phys. Lett.* **91**, 113512 (2007).
- [76] It is worth to mention that for an in-plane exchange field as is shown in Fig. 1 the Rashba SO coupling by itself does not generate long-range triplet correlations at S/F interfaces. Therefore, to produce them spin-active layers should be added to the system at the S/F interfaces. However, this problem is widely studied in the literature[5, 8, 9] and is not discussed here.